Surgical and Radiologic Anatomy (2019) 41:785–789
https://doi.org/10.1007/s00276-019-02216-9

ORIGINAL ARTICLE

Anatomical–positional relationship between the bone structure of the distal radius and flexor pollicis longus tendon using ultrasonography

Mayuko Kinoshita[1] · Kiyohito Naito[1] · Kenji Goto[1] · Yoichi Sugiyama[1] · Nana Nagura[1] · Hiroyuki Obata[1] · Yoshiyuki Iwase[2] · Kazuo Kaneko[1]

Received: 29 December 2018 / Accepted: 9 March 2019 / Published online: 16 March 2019
© Springer-Verlag France SAS, part of Springer Nature 2019

Abstract

Purpose In this study, using an ultrasonography, we investigated the positional relationship between the volar bone cortex of distal radius and flexor pollicis longus (FPL) tendon in the distal radius of healthy subjects.

Methods The subjects were 32 healthy volunteers (56 wrists) (Age 32.9 ± 8.5, 16 males and 16 females). Their wrists were imaged by an ultrasonography. The distances between the watershed line (WS) and FPL (A), between the distal margin of pronator quadratus (DMPQ) and FPL (B), between the FPL and volar radial bone cortex at the maximum muscle belly of the PQ muscle right below the sliding region of the FPL tendon (C), and between the WS and DMPQ (D) were measured.

Results All these parameters showed a normal distribution. When the correlation among the parameters was investigated, a correlation with an index of the physique, BMI, was noted in A ($P < 0.01$), B ($P < 0.01$), and C ($P < 0.01$), but no correlation was noted only in D ($P = 0.59$).

Conclusions Our results were suggested that when distal radius fracture is treated with a distal plate placement, the appropriate placement can be achieved by applying about 3 mm additional dissection of soft tissue on the volar bone cortex distal to the DMPQ.

Keywords Distal radius fracture · Flexor pollicis longus tendon · Ultrasonography · Bone structure of the distal radius

Introduction

Distal radius fracture is a trauma frequently encountered in routine medical practice [1] and osteosynthesis using a volar locking plate has recently been increasing for its treatment [14]. However, attention should be always paid to complications of a volar locking plate because it is placed on the bone surface. Injury of the flexor pollicis longus (FPL) tendon markedly reduces the level of daily life and postoperative outcome of the patient and this is recognized as a complication requiring preventive measures because the incidence is about 5%, being not negligible for orthopaedic surgeons [7, 11, 12, 15].

The cause of FPL injury is the design or placement position of the plate in many cases [1, 12]. The plate is placed between the bone cortex of the volar distal radius and FPL tendon, but it is considered that degenerative rupture of the tendon is caused by interference with the placed plate by the FPL tendon [1, 12]. Thus, we considered that thorough understanding of the anatomical relationship between the bone structure of the volar distal radius on which the plate is placed and FPL tendon is necessary to prevent FPL tendon injury after plate placement. In this study, using an ultrasonography, we investigated the positional relationship between the volar bone cortex of distal radius and FPL tendon in the distal radius of healthy subjects and discussed careful points of plate placement based on the clarified positional relationship.

✉ Kiyohito Naito
knaito@juntendo.ac.jp

1 Department of Orthopaedics, Juntendo University School of Medicine, 1-5-29 Yushima, Bunkyo-ku, Tokyo 113-0034, Japan

2 Department of Orthopaedic Surgery, Juntendo Tokyo Koto Geriatric Medical Center, 3-3-20 Shinsuna, Koto-ku, Tokyo 136-0075, Japan

Materials and methods

The study was approved by the Ethics Committee for Medical Research of our university (No. 18-054), and informed consent was obtained from all volunteers.

The Japanese subjects were 16 healthy male volunteers (26 wrist joints) and 16 healthy female volunteers (30 wrist joints) with no past medical history of trauma or complaint of the wrist joint (56 wrist joints in total, 26 in male and 30 in female; mean age: 32.9 ± 8.5). Six wrists in male and two wrists in female were excluded in this study due to past traumatic history. Measurement was performed by one orthopaedic surgeon using ultrasonography, Venu 40 (frequency 60 Hz, GH Health Care, Tokyo, Japan), a 12 MHz probe, and B-mode. To uniform the force pressing the probe to the skin, the probe was attached lightly so as to remain a single layer of jelly in the visualized image.

The measurement position was set at the maximum supination of the forearm with 20° dorsiflexion of the wrist joint and finger extension following that reported by Nanno et al. (Fig. 1a) [8]. The thumb was maintained in 45° radial abduction and IP joint of the thumb was mainteined in extension position following that reported by Tanaka et al. (Fig. 1a) [12]. At first, to define the direction of the visualized laminar arrangement of linear high echo (fibrillary pattern) in the tendon as the long axis direction of the FPL tendon, the ultrasound probe was set in this direction (Fig. 1b). Next, the most protruding region of the osteal prominence of the distal radius right below the sliding region of the FPL tendon as watershed line (WS) and the pronator quadratus muscle attachment site of the distal radius right below the sliding region of the FPL tendon as the distal margin of pronator quadratus (DMPQ) were defined. Then, the distances between the WS and FPL (A), between the DMPQ and FPL (B), between the FPL and volar radial bone cortex at the maximum muscle belly of the pronator quadratus muscle (PQ) right below the sliding region of the FPL tendon (C), and between the WS and DMPQ (D) were measured (Fig. 2). Measurement was repeated three times by same orthopaedic surgeon and the mean was calculated and subjected to statistical analysis. The intra-observer agreements for the measurement of A–D were assessed using the intraclass correlation coefficient (ICC) calculated. The body mass index (BMI) of subjects was also investigated as an index of physique.

Data were presented as the mean ± standard deviation (SD) or 95% confidence interval. In statistical analysis, correlation and linear regression analyses were performed using IBM SPSS (Ver.22.0.0). Differences were considered statistically significant at $P < 0.05$.

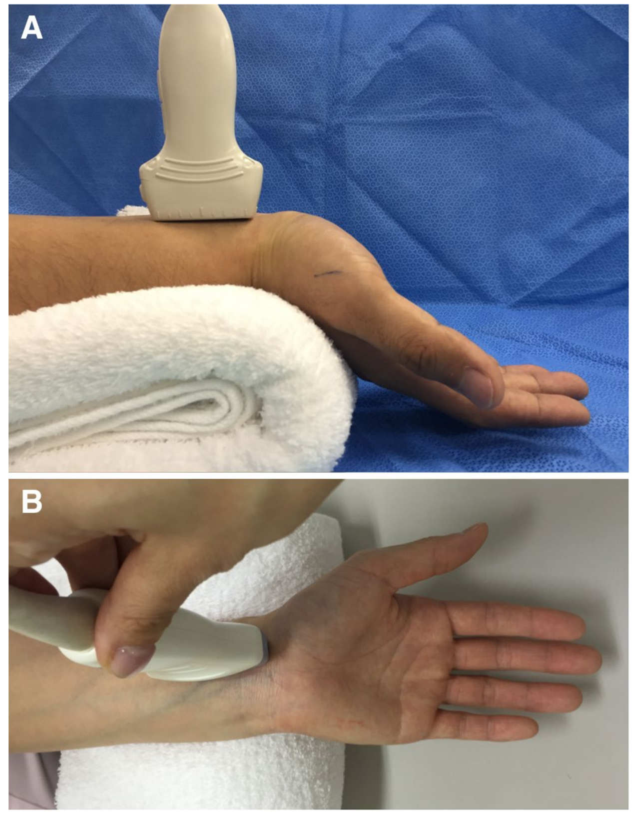

Fig. 1 Position for measurement using the ultrasonography. **a** The measurement was performed in a position set at the maximum supination with 20° dorsiflexion of the wrist joint and finger extension. **b** Defining the direction of the visualized laminar arrangement of linear high echo (fibrillary pattern) in the tendon as a long axis direction of the FPL tendon, the ultrasound probe was set in the long axis direction of the FPL tendon

Results

Regarding the patient background, the age was 23–55 years old (mean 32.6 ± 6.9), and BMI was 16.2–29.4 kg/m^2 (mean 21.2 ± 3.2).

The anatomical relationship between the bone structure of the volar distal radius and FPL tendon measured using ultrasonography was as follows:

- A: Distance between the WS and FPL

WS represents the osteal prominence visualized right below the sliding region of the FPL in the long axis view on ultrasonography. The distance between this WS and FPL was measured. The mean distance was 1.7 mm (95% confidence interval: 0.6–2.8 mm) (Fig. 2). ICC for intra-observer agreement was 0.97 (95% confidence interval 0.96–0.98).

- B: Distance between the DMPQ and FPL

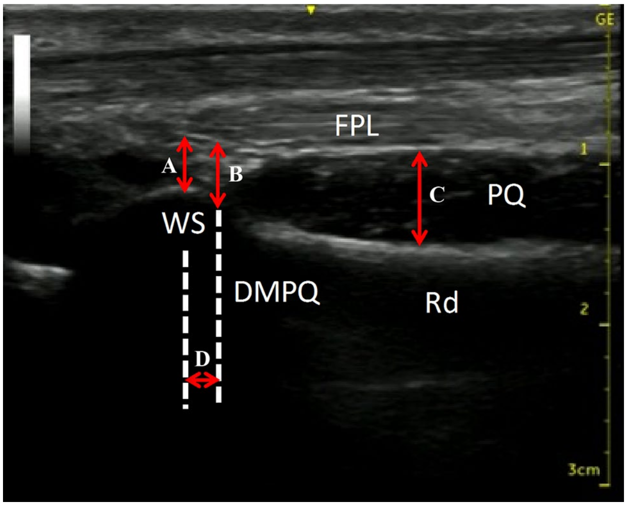

Fig. 2 Actual ultrasound images and definitions of measurement parameters. The most protruding region of the osteal prominence of the distal radius right below the sliding region of the FPL tendon was defined as the watershed line (WS), and the pronator quadratus muscle (PQ) attachment site of the distal radius right below the sliding region of the FPL tendon was defined as the distal margin of pronator quadratus (DMPQ). The following four parameters were measured: **a** distance between the WS and FPL, **b** distance between DMPQ and FPL, **c** distance between FPL and volar radial bone cortex at the maximum muscle belly of the PQ right below the sliding region of the FPL tendon, **d** distance between the WS and DMPQ

The DMPQ was visualized right below the sliding region of the FPL in the long axis view on ultrasonography. The distance between this DMPQ and FPL was measured. The mean distance was 3.1 mm (95% confidence interval 1.5–4.7 mm) (Fig. 2). ICC for intra-observer agreement was 0.94 (95% confidence interval 0.92–0.97).

- C: Distance between the FPL and the radius at the maximum muscle belly of the PQ

The distance between the radius and FPL at the maximum muscle belly of the PQ right below the FPL sliding region in the long axis view on ultrasonography was measured. The mean distance was 5.1 mm (95% confidence interval 1.5–8.7 mm) (Fig. 2). ICC for intra-observer agreement was 0.96 (95% confidence interval 0.95–0.98).

- D: Distance between the WS and DMPQ

The vertical distance between the WS and DMPQ visualized right below the sliding region of the FPL in the long axis view on ultrasonography was measured. The mean distance was 3.3 mm (95% confidence interval 0.9–5.7 mm) (Fig. 2). ICC for intra-observer agreement was 0.97 (95% confidence interval 0.96–0.98).

All these parameters showed a normal distribution. When the correlation among the parameters was investigated, a correlation with an index of the physique, BMI, was noted in A: WS-FPL ($P<0.01$, Fig. 3a), B: DMPQ-FPL ($P<0.01$, Fig. 3b), and C: Rd-FPL ($P<0.01$, Fig. 3c), but no correlation was noted only in D: WS-DMPQ ($P=0.59$, Fig. 3d). It was clarified by linear regression analyses between BMI and these parameters that the index of physique, BMI, may be an explanatory variable for A: WS-FPL ($R^2=0.27$, Fig. 3a), B: DMPQ-FPL ($R^2=0.26$, Fig. 3b), and C: Rd-FPL ($R^2=0.16$, Fig. 3c). D: WS-DMPQ was constantly 3.3 mm regardless of the physique ($R^2=0.01$, Fig. 3d).

Discussion

WS was defined as the transverse ridge bordering the pronator fossa distally by Orbay and Touhami in 2006 and proposed as an osteal index utilized to decide on the optimum placement position of a volar locking plate for distal radius fracture [10], and Cross et al. reported that the risk of flexor tendon injury may increase when a volar locking plate is placed at a site across the WS [2]. However, the definition of the WS is vague. In 2012, Imatani et al. performed anatomical analysis using frozen cadavers and reported that the WS might not be a distinct line, and it corresponds to the distal margin of the pronator fossa in the lateral half of the volar radius and to a hypothetical line between the distal and proximal lines in the medial half [4]. They concluded that the osteal prominence is different between the medial and lateral sides and the osteal prominence cannot be connected by a single line [4], suggesting that the volar locking plate placement position cannot be decided based on the osteal prominence alone as an index. Moreover, Kwon et al. suggested that considerable variability exists in the morphometry of the volar distal radius, with sex and race as contributing factors [6]. In the present study, the distance between the DMPQ and WS was constant regardless of the physique and the mean distance was 3.3 mm (95% confidence interval 0.9–5.7 mm). Therefore, it was suggested that appropriate volar locking plate placement can be achieved by applying about 3 mm additional dissection of soft tissue on the volar bone cortex toward the distal side setting the baseline at the DMPQ.

Regarding the volar locking plate placement position and friction during sliding of the FPL tendon, Tanaka et al. investigated these in frozen cadavers and clarified that the friction force loaded on the flexor tendon increased as the plate placement position moved toward the distal side, and when the plate was placed at a site across the WS, the friction force reached the maximum [12]. When friction between the osteal prominence right below the FPL sliding region, which is the nearest to the FPL, and the FPL was

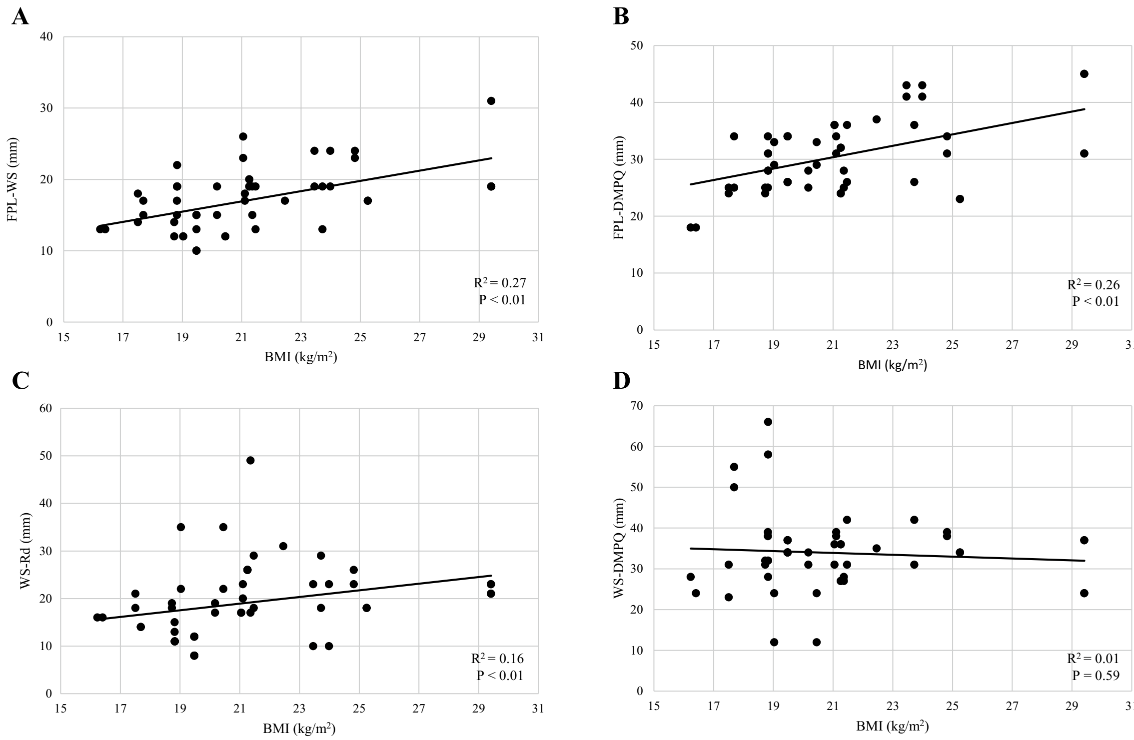

Fig. 3 Correlations between parameters and BMI. **a** A positive correlation with BMI was noted in the distance between the WS and FPL, and an influence on BMI was detected on linear regression analysis ($R^2=0.27$, $P<0.01$). **b** A positive correlation with BMI was noted in the distance between the DMPQ and FPL, and an influence on BMI was detected on linear regression analysis ($R^2=0.26$, $P<0.01$). **c** A positive correlation with BMI was noted in the distance between the FPL and volar radial bone cortex at the maximum muscle belly of PQ right below the sliding region of the FPL tendon and an influence on BMI was detected on linear regression analysis ($R^2=0.16$, $P<0.01$). **d** No correlation with BMI was noted in the distance between the WS and DMPQ, and BMI was not influenced on linear regression analysis ($R^2=0.01$, $P=0.59$)

investigated without placing a volar locking plate, the friction force was 0 N/cm^2, demonstrating that plate placement increased friction loaded on FPL and the risk for friction-induced flexor tendon rupture, and distal plate placement further increases this risk. In our study, the distance between the WS and FPL was influenced by the physique, but the mean was 1.7 mm (95% confidence interval 0.6–2.8 mm), being close, the mean distance between the DMPQ and FPL was 3.1 mm (95% confidence interval 1.5–4.7 mm), and that between the radius and FPL at the maximum muscle belly of the PQ was 5.1 mm (95% confidence interval 1.5–8.7 mm), showing that the plate is placed in a narrow space. Thus, pressure joining the plate to the radius is important, i.e., it was suggested that plate placement may exclude the FPL and change the FPL sliding position. To avoid the irritation between FPL tendon and volar locking plate, it will be necessary to repair a pronator quadratus muscle [3].

Ultrasonography is an imaging diagnosis tool with diverse possibilities and anatomical structures can be evaluated noninvasively and easily using it. In rheumatoid arthritis, inflammation is evaluated based on the blood flow volume using the Doppler function of ultrasonography. It is also capable of dynamic evaluation, such as evaluation of tendon sliding as observed in this study. Differences in the friction force loaded on the tendon depending on the finger and wrist joint movements have been reported [12], suggesting that the merit of dynamic evaluation is large to examine the tendon. In fact, the research on imaging diagnosis using ultrasonography for the prevention and early detection of FPL tendon damage after volar locking plate fixation for the distal radius fractured has been conducted and its feasibility has been reported from several researchers in recent years [5, 9, 13].

There are several limitations of this study. Firstly, the number of samples was small. The normal structure of the distal radius was evaluated using ultrasonography, but differences in the structure among wide age groups by increasing the sample number remain to be investigated. Secondly, the wrist joint was set at a specified position. Since the flexor tendon distribution changes due to not only movement of the fingers, but also flexion/extension of the wrist joint, investigation at various positions may be required. Finally, no comparative group was set. Comparison of the evaluation with that in a patient group with plate placement is significant for prevention of complications of distal radius fracture treatment in the future. However, evaluation of implant placement using ultrasound is difficult, for which investigation of another evaluation method is necessary.

Conclusion

The anatomical positional relationship between the FPL and distal radius could be evaluated noninvasively using ultrasonography. The distance between the WS and DMPQ was not influenced by the physique and it was short (about 3 mm). It was suggested that when distal radius fracture is treated with a distal plate placement, the appropriate placement can be achieved by applying about 3 mm additional dissection of soft tissue on the volar bone cortex distal to the DMPQ.

Author contributions Protcol/project development was performed by KN and YI. Data collection or management was performed by MK, KG, YS, HO, and NN. Data analysis was performed by MK, KG, YS, HO, NN, and KN. Manuscript writing/editing was performed by MK, KK, and KN.

Compliance with ethical standards

Conflict of interest The authors declare that they have no conflict of interest.

References

1. Asadollahi S, Keith PP (2013) Flexor tendon injuries following plate fixation of distal radius fractures: a systematic review of the literature. J Orthop Traumatol 14:227–234
2. Cross AW, Schmidt CC (2008) Flexor tendon injuries following locked volar plating of distal radius fractures. J Hand Surg Am 33:164–167
3. Goorens CK, Van Royen K, Grijseels S, Provyn S, De Mey J, Scheerlinck T, Goubau JF (2018) Ultrasonographic evaluation of the distance between the flexor pollicis longus tendon and volar prominence of the plate as a function of volar plate positioning and pronator quadratus repair—a cadaver study. Hand Surg Rehabil 37:171–174
4. Imatani J, Akita K, Yamaguchi K, Shimizu H, Kondou H, Ozaki T (2012) An anatomical study of the watershed line on the volar, distal aspect of the radius: implications for plate placement and avoidance of tendon ruptures. J Hand Surg Am 37:1550–1554
5. Kadoma C, Takahara M, Maruyama M, Satake H, Takagi M (2017) Ultrasonographic assessment of the flexor pollicis longus tendon after plate fixation. Orthopedics 40:e104–e108
6. Kwon BC, Lee JK, Lee SY, Hwang JY, Seo JH (2018) Morphometric variations in the volar aspect of the distal radius. Clin Orthop Surg 10:462–467
7. Limthongthang R, Bachoura A, Jacoby SM, Osterman AL (2014) Distal radius volar locking plate design and associated vulnerability of the flexor pollicis longus. J Hand Surg Am 39:852–860
8. Nanno M, Kodera N, Tomori Y, Takai S (2016) Transverse ultrasound assessment of the flexor pollicis longus tendon movement on the distal radius during wrist and finger motion in distal radius fracture with volar plating. J Med Ultrason (2001) 43:29–36
9. Nanno M, Kodera N, Tomori Y, Takai S (2018) Ultrasonographic movement of the flexor pollicis longus tendon before and after removal of a volar plate for the distal radius fracture. J Orthop Surg 26:2309499018760131
10. Orbay JL, Touhami A (2006) Current concepts in volar fixed-angle fixation of unstable distal radius fractures. Clin Orthop Relat Res Apr 445:58–67
11. Soong M, van Leerdam R, Guitton TG, Got C, Katarincic J, Ring D (2011) Fracture of the distal radius: risk factors for complications after locked volar plate fixation. J Hand Surg Am 36:3–9
12. Tanaka Y, Aoki M, Izumi T, Fujimiya M, Yamashita T, Imai T (2011) Effect of distal radius volar plate position on contact pressure between the flexor pollicis longus tendon and the distal plate edge. J Hand Surg Am 36:1790–1797
13. Tanaka Y, Gotani H, Yano K, Sasaki K, Hamada Y (2017) Evaluation of flexor pollicis longus tendon attrition using color Doppler imaging after volar plate fixation for distal radius fracture. J Orthop Sci 22:447–452
14. Vosbikian MM, Ketonis C, Huang R, Ilyas AM (2016) Optimal positioning for volar plate fixation of a distal radius fracture: determining the distal dorsal cortical distance. Orthop Clin N Am 47:235–244
15. Yamazaki H, Uchiyama S, Komatsu M, Hashimoto S, Kato H (2015) Risk assessment of tendon attrition following treatment of distal radius fractures with volar locking plates using audible crepitus and placement of the plate: a prospective clinical cohort study. J Hand Surg Am 40:157–181

Publisher's Note Springer Nature remains neutral with regard to jurisdictional claims in published maps and institutional affiliations.